ISSN 3048-8222 (Online) | www.ijsate.com | editor@ijsate.com



International Journal of
Science, Architecture, Technology and Environment

Improving Estimation and Control Accuracy of Underwater Vehicle Dynamics Using the Extended Kalman Filter and Sliding Mode Control

Ngo Trung Toan[1*], Dao Thanh Bang[1]

[1]*Missile Faculty, Air Defence-Air Force Academy, Ha Noi, Viet Nam*

[*]*Corresponding author email: Huyndai55@gmail.com*

DOI: https://doi.org/10.63680/ijsate0226014.010

Abstract

This paper proposes a method that combines the Extended Kalman Filter (EKF) with Sliding Mode Control (SMC) in order to improve the accuracy of estimation and control of the dynamic parameters of a 12-degree-of-freedom (12 DOF) underwater vehicle. A complete nonlinear dynamic model of the vehicle is developed, taking into account environmental effects including ocean waves, currents, and disturbances. EKF is employed to accurately estimate position, velocity, Euler angles, and angular rates even when measurement signals are corrupted by Gaussian noise. Meanwhile, the sliding mode controller is applied to the depth and pitch control channels, in combination with a PD controller for the yaw channel, ensuring fast response and robustness against external disturbances and parameter variations. Simulation results show that the proposed method significantly reduces estimation error, maintains system stability, and limits control energy compared to traditional methods.

Keywords: Underwater vehicle, 12 DOF, EKF, Extended Kalman Filter, SMC, Sliding Mode Control, robust control, marine environmental disturbance.

1. Introduction

Autonomous Underwater Vehicles (AUVs) play a crucial role in ocean exploration, search and rescue, and deep-sea research missions. Accurate control of AUVs is a major challenge due to their complex dynamics, strongly influenced by marine environmental factors such as waves, currents, and unknown disturbances. In particular, 12-DOF vehicles have a large number of state variables, strong nonlinearities, and cross-coupling among control channels, making the estimation and control problem highly challenging.

In classical control methods, the EKF is often used to estimate states from noisy measurements. However, its capability to compensate disturbances and cope with parameter variations is limited. On the other hand, SMC is well known for its robustness and strong disturbance rejection capability, but it may induce control chattering and requires accurate state estimation.

To overcome these limitations, this paper proposes combining EKF and SMC for the estimation and

ISSN 3048-8222 (Online) | www.ijsate.com | editor@ijsate.com

control of 12-DOF underwater vehicle dynamics. The EKF ensures accurate state estimation even with noisy measurements, while SMC enables the system to maintain stability and follow reference trajectories under harsh environmental conditions. The proposed method is validated through simulations under wave disturbances, current effects, and random drag forces, showing superior performance in terms of both accuracy and robustness.

2. Algorithm Synthesis

- Consider the state vector of the underwater vehicle:

$$x(t) = \begin{bmatrix} x & y & z & v_x & v_y & v_z & \phi & \theta & \psi & p & q & r \end{bmatrix}^T \quad (1)$$

Where:

x, y, z : positions in the inertial frame (m);

v_x, v_y, v_z : linear velocities in the vehicle frame (m/s);

ϕ, θ, ψ : Euler angles (roll, pitch, yaw) (rad);

p, q, r : angular rates around the vehicle body axes (rad/s).

- Control vector:

$$u(t) = \begin{bmatrix} u_{heave}(t) & u_{pitch}(t) & u_{yaw}(t) \end{bmatrix}^T \quad (2)$$

Where:

u_{heave} : control force along the z-axis of the body frame (N);

u_{pitch} : control moment about the y-axis (N.m);

u_{yaw} : control moment about the z-axis (N.m).

- Environmental disturbance vector:

$$\mathrm{w}(t) = \begin{bmatrix} \mathrm{w}_{wave}(t) & \mathrm{w}_{\mathrm{current}}(t) & \mathrm{w}_{\rho}(t) \end{bmatrix}^T \quad (3)$$

Where:

w_{wave} : disturbance due to waves (m);

$\mathrm{w}_{\mathrm{current}}$: disturbance due to currents (m/s);

w_{ρ} : random disturbance (N).

- General 12-DOF state equation:

$$\dot{x}(t) = f(x(t)) + B_u u(t) + B_{\mathrm{W}} \mathrm{w}(t) \quad (4)$$

Where:

$f(x(t))$: nonlinear vector function describing natural kinematics and dynamics of the vehicle;

B_u : control distribution matrix (size 12×3);

B_{W} : environmental disturbance distribution matrix (size 12×3).

- From (4) the system of differential equations for each state:

$$\dot{x} = v_x, \dot{y} = v_y, \dot{z} = v_z \quad (5)$$

$$\dot{v}_x = -\frac{d_{lin}}{m} v_x + k_{cx} \mathrm{w}_{\mathrm{current}} \quad (6)$$

$$\dot{v}_y = -\frac{d_{lin}}{m} v_y \quad (7)$$

ISSN 3048-8222 (Online) | www.ijsate.com | editor@ijsate.com

$$\dot{v}_z = -\frac{d_{lin}}{m} v_z - k_g \theta + k_{\mathrm{wz}} \mathrm{w}_{wave} + \frac{\mathrm{w}_\rho + u_{heave}}{m} \tag{8}$$

$$\dot{\phi} = p, \dot{\theta} = q, \dot{\psi} = r \tag{9}$$

$$\dot{p} = -\frac{d_{ang}}{I_{xx}} p + k_{cp} \mathrm{w}_{\mathrm{current}} \tag{10}$$

$$\dot{q} = -\frac{d_{ang}}{I_{yy}} q - k_t \theta + k_{\mathrm{wq}} \mathrm{w}_{wave} + \frac{u_{pitch}}{I_{yy}} \tag{11}$$

$$\dot{r} = -\frac{d_{ang}}{I_{zz}} r - c_\psi \psi + k_{cr} \mathrm{w}_{\mathrm{current}} + k_{\mathrm{wr}} \mathrm{w}_{wave} + \frac{u_{yaw}}{I_{zz}} \tag{12}$$

Where:

m : mass of the vehicle (kg);

I_{xx}, I_{yy}, I_{zz} : moments of inertia about the body axes (kg.m^2);

d_{lin} : linear drag coefficient (N.s/m);

d_{ang} : rotational drag coefficient (N.m.s/rad);

k_g : gravitational effect coefficient on the z channel (m/s^2);

c_ψ : yaw restoring stiffness coefficient (N.m/rad);

k_{cx}, k_{cp}, k_{cr} : current disturbance coefficients on the respective equations;

k_t : stiffness coefficient with respect to θ ;

$k_{\mathrm{wz}}; k_{wq}; k_{\mathrm{wr}}$: wave disturbance coefficients on the respective equations.

To accurately estimate the vehicle states under noisy measurements and significant marine disturbances, the EKF is employed. EKF handles nonlinear systems by locally linearizing around the current state estimate, combining model predictions with actual measurements to reduce estimation errors. This process includes two main stages:

Prediction step – predicting states and covariance based on the discretized model of the 12-DOF system.

Update step – updating using measurements [z, θ, q, ψ] and the corresponding measurement matrix.

- Discretization of the model and EKF estimation for 12 DOF :

With sampling period $T_s > 0$, applying forward Euler discretization to (4):

$$x_{k+1} = x_k + T_s f(x_k) + B_u u_k + B_{\mathrm{w}} \mathrm{w}_k + G q_k \tag{13}$$

$$y_k = H x_k + v_k \tag{14}$$

T_s : sampling period (s);

$q_k \sim N(0, Q)$: process noise;

$v_k \sim N(0, R)$: measurement noise;

G : process noise distribution matrix;

H : measurement matrix selecting [z, θ, q, ψ] components from x (size 4×12).

- EKF Linearization for 12 DOF:

At $\hat{\mathrm{x}}_{k|k}$ Jacobian of f is:

$$F_k = \left.\frac{\partial f}{\partial x}\right|_{\hat{\mathrm{x}}_{k|k}}, F_{d,k} = I_{12} + T_s F_k \tag{15}$$

ISSN 3048-8222 (Online) | www.ijsate.com | editor@ijsate.com

The covariance prediction is updated using the first-order discrete approximation:

$$P_{k|k+1} = F_{d,k} P_{k|k} F_{d,k}^T + Q \tag{16}$$

- Prediction of 12 State Variables, from (5)–(12), the prediction step of EKF (forward Euler) becomes:

$$\hat{\mathrm{x}}_{k+1|k} = \hat{\mathrm{x}}_{k|k} + T_s \hat{v}_x \tag{17}$$

$$\hat{y}_{k+1|k} = \hat{y}_{k|k} + T_s \hat{v}_y \tag{18}$$

$$\hat{z}_{k+1|k} = \hat{z}_{k|k} + T_s \hat{v}_z \tag{19}$$

$$\hat{v}_{x,k+1|k} = \hat{v}_{x,k|k} + T_s(-\frac{d_{lin}}{m}\hat{v}_{x,k|k} + k_{cx}\mathrm{w}_{\mathrm{current}}) \tag{20}$$

$$\hat{v}_{y,k+1|k} = \hat{v}_{y,k|k} + T_s(-\frac{d_{lin}}{m}\hat{v}_{y,k|k}) \tag{21}$$

$$\hat{v}_{z,k+1|k} = \hat{v}_{z,k|k} + T_s(-\frac{d_{lin}}{m}\hat{v}_{z,k|k} - k_g\theta + k_{\mathrm{wz}}\mathrm{w}_{wave} + \frac{\mathrm{w}_\rho + u_{heave}}{m}) \tag{22}$$

$$\hat{\phi}_{k+1|k} = \hat{\phi}_{k|k} + T_s \hat{p}_{k|k} \tag{23}$$

$$\hat{\theta}_{k+1|k} = \hat{\theta}_{k|k} + T_s \hat{q}_{k|k} \tag{24}$$

$$\hat{\psi}_{k+1|k} = \hat{\psi}_{k|k} + T_s \hat{r}_{k|k} \tag{25}$$

$$\hat{p}_{k+1|k} = \hat{p}_{k|k} + T_s(-\frac{d_{ang}}{I_{xx}}\hat{p}_{k|k} + k_{cp}\mathrm{w}_{\mathrm{current}}) \tag{26}$$

$$\hat{q}_{k+1|k} = \hat{q}_{k|k} + T_s(-\frac{d_{ang}}{I_{yy}}\hat{q}_{k|k} - k_t\theta + k_{\mathrm{wq}}\mathrm{w}_{wave} + \frac{u_{pitch}}{I_{yy}}) \tag{27}$$

$$\hat{r}_{k+1|k} = \hat{r}_{k|k} + T_s(-\frac{d_{ang}}{I_{zz}}\hat{r}_{k|k} - c_\psi\psi + k_{cr}\mathrm{w}_{\mathrm{current}} + k_{\mathrm{wr}}\mathrm{w}_{wave} + \frac{u_{yaw}}{I_{zz}}) \tag{28}$$

- Measurement Update:

$$y_k = \begin{bmatrix} z_k \\ \theta_k \\ q_k \\ \psi_k \end{bmatrix} = Hx_k + v_k \tag{29}$$

- Innovation Error (with yaw angle wrapping):

$$\tilde{y}_k = \begin{bmatrix} z_k - \hat{z}_{k|k-1} \\ \theta_k - \hat{\theta}_{k|k-1} \\ q_k - \hat{q}_{k|k-1} \\ \mathrm{W}\psi_k - \hat{\psi}_{k|k-1} \end{bmatrix} \tag{30}$$

Where W(·) denotes the wrapping of the yaw angle into the interval (−π,π].

- Kalman Gain and Update:

Innovation covariance:

$$S_k = HP_{k|k-1}H^T + R \tag{31}$$

Kalman gain:

$$K_k = P_{k|k-1}H^T S_k^{-1} \tag{32}$$

ISSN 3048-8222 (Online) | www.ijsate.com | editor@ijsate.com

State update:

$$\hat{x}_{k|k} = \hat{x}_{k|k-1} + K_k \tilde{y}_k \quad (33)$$

Covariance update:

$$P_{k|k} = (I_{12} - K_k H) P_{k|k-1} \quad (34)$$

- The four directly measured variables are updated as:

$$\hat{z}_{k|k} = \hat{z}_{k|k-1} + k_k^{(z)} \tilde{y}_k \quad (35)$$

$$\hat{\theta}_{k|k} = \hat{\theta}_{k|k-1} + k_k^{(\theta)} \tilde{y}_k \quad (36)$$

$$\hat{q}_{k|k} = \hat{q}_{k|k-1} + k_k^{(q)} \tilde{y}_k \quad (37)$$

$$\hat{\psi}_{k|k} = \mathrm{W}\hat{\psi}_{k|k-1} + k_k^{(\psi)} \tilde{y}_k \quad (38)$$

Where $k_k^{(i)}$ is the corresponding row of K_k (size 1x4).

- The eight unmeasured states are corrected indirectly due to correlations in the covariance matrix P:

$$\hat{x}_{k|k} = \hat{x}_{k|k-1} + k_k^{(\chi)} \tilde{y}_k, \chi \in \{x, y, v_x, v_y, v_z, \phi, p, r\} \quad (39)$$

Based on the estimated states from the Extended Kalman Filter, controllers are designed to ensure the 12-DOF underwater vehicle tracks reference trajectories under harsh marine environments. The design principle is to separate control channels according to their dynamics:

Depth (z) and pitch (θ) channels exhibit strong nonlinearities and are subject to large disturbances → SMC is applied for robustness and disturbance rejection.

Yaw (ψ) channel has simpler dynamics → a Proportional-Derivative (PD) controller is used to achieve fast response and reduced oscillations.

- Sliding Mode Control (SMC) for Depth z and Pitch θ:

+ Error and error derivative:

$$e_z(k) = z_{ref}(k) - \hat{z}_{k|k}; \quad \dot{e}_z(k) \approx \frac{e_z(k) - e_z(k-1)}{T_s} \quad (40)$$

$$e_\theta(k) = \theta_{ref}(k) - \hat{\theta}_{k|k}; \quad \dot{e}_\theta(k) \approx \frac{e_\theta(k) - e_\theta(k-1)}{T_s} \quad (41)$$

+ Sliding surfaces:

$$s_z(k) = \lambda_z e_z(k) + \lambda_1 \dot{e}_z(k) \quad (42)$$

$$s_\theta(k) = \lambda_\theta e_\theta(k) + \lambda_1 \dot{e}_\theta(k) \quad (43)$$

+ SMC control laws:

$$u_{heave}(k) = K_{fb,z}(e_z(k) + k_{ez}\dot{e}_z(k)) - K_z \,\mathrm{sgn}(s_z(k)) \min(1, \frac{|s_z(k)|}{\phi_z}) \quad (44)$$

$$u_{pitch}(k) = K_{fb,\theta}(\lambda_\theta e_\theta(k) + \lambda_z \dot{e}_\theta(k)) - K_\theta \,\mathrm{sgn}(s_\theta(k)) \min(1, \frac{|s_\theta(k)|}{\phi_\theta}) \quad (45)$$

z_{ref} : reference depth (m);

θ_{ref} : reference pitch angle (rad);

$\hat{z}$: depth estimated by EKF (m);

$\hat{\theta}$: pitch angle estimated by EKF (rad);

$\lambda_z, \lambda_\theta, \lambda_1$: sliding surface coefficients (1/s);

ISSN 3048-8222 (Online) | www.ijsate.com | editor@ijsate.com

$K_{fb,z}, K_{fb,\theta}$: linear feedback gains (N/m);

k_{ez} : proportional coefficients for error derivative (s);

K_z, K_θ : sliding gain coefficients (N), (N/m);

ϕ_z, ϕ_θ : boundary layer values to reduce chattering (m), (rad);

sgn(.) : sign function.

- PD Control for Yaw ψ :

Yaw error:

$$e_\psi(k) = \mathrm{W}\psi_{ref}(k) - \hat{\psi}_{k|k} \tag{46}$$

Control law:

$$u_{yaw}(k) = K_{p,\psi} e_\psi(k) - K_{d,\psi} \hat{r}_{k|k} \tag{47}$$

ψ_{ref} : reference yaw angle (rad);

$\hat{\psi}$: EKF estimated yaw (rad);

$\hat{r}$: estimated yaw rate (rad/s);

$K_{p,\psi}$: proportional gain (N·m/rad);

$K_{d,\psi}$: derivative gain (N·m·s/rad).

- All control inputs are subject to actuator limits:

$$u_{\min} \le u_{heave}, u_{pitch}, u_{yaw} \le u_{\max} \tag{48}$$

u_{heave} : heave control force (N);

u_{pitch} : pitch control moment (N.m);

u_{yaw} : yaw control moment (N.m).

3. Simulation and Evaluation

In this section, the adaptive filtering algorithm based on the posterior density is tested using numerical simulation. The dynamic system consists of three states $[R, V, W]^T$, where the true values are generated using the Euler–Maruyama method with diffusion noise dependent on the parameter α . The filter performs two processes: state estimation using a linearized Kalman-type structure with respect to matrix c , and updating the two unknown parameters α and λ based on the observation residual and model deviation. Dynamic constraints are applied to ensure stability and prevent parameter drift. The simulation results present the convergence of the states, parameters, trace $D(x)$ as well as the RMSE, innovation, and Kalman-type gain components.

To verify the effectiveness of the EKF combined with SMC and PD yaw controller in state estimation and control of the 12-DOF underwater vehicle, the dynamic and control models are implemented according to the established equations, considering disturbances from waves, currents, and random perturbations. Reference signals for depth, pitch, and yaw channels are either fixed or time-varying to evaluate tracking performance. The simulation parameters are chosen as follows:

- Sampling period: 0.01 (s); simulation time: 30 (s);
- Vehicle mass: 5000 (kg), moments of inertia: $I_{xx} = 50$ (kg/m^2), $I_{yy} = 60$ (kg/m^2), $I_{zz} = 80$ (kg/m^2).
- Linear drag coefficient: $d_{lin} = 50$ (N.s/m), angular drag coefficient: $d_{ang} = 25$ (N.m.s/rad).

ISSN 3048-8222 (Online) | www.ijsate.com | editor@ijsate.com

- Control limits: $u_{heave} \in [-150,150]$ (N); $u_{pitch} \in [-80,80]$ (N.m); $u_{yaw} \in [-50,50]$ (N.m).

- SMC parameters. Depth: $\lambda_z = 2; \phi_z = 0.06; K_z = 160; K_{fb,z} = 120$; Pitch: $\lambda_\theta = 3; \phi_\theta = 0.03; K_\theta = 60; K_{fb,\theta} = 30$; Additional coefficient: $\lambda_1 = 1.5$; PD yaw controller: $K_{p,\psi} = 30; K_{d,\psi} = 8$.

- Environmental disturbances. Wave: amplitude 0.4(m), frequency 0.12(Hz), sinusoidal form; Current: amplitude 0.15(m/s), frequency 0.015(Hz), random form. Random disturbance: amplitude 1.5(N), frequency 0.005(Hz), sinusoidal form.

- External disturbance: a force of 50(N) applied on the z-axis during 6–7.5(s).

- EKF configuration:

+ Initial covariance matrix:

$$P_0 = diag(0.5,\ 0.5,\ 0.5, 0.2, 0.2, 0.2,\ 0.05, 0.05,\ 0.1, 0.02, 0.02, 0.1)$$

+ Process noise covariance:

$$Q = diag(10^{-3}, 10^{-3}, 10^{-3}, 10^{-2}, 10^{-2}, 10^{-2}, 5.10^{-4}, 5.10^{-4}, 2.10^{-3}, 5.10^{-4}, 5.10^{-4}, 2.10^{-3})$$

+ Measurement noise covariance:

$$R = diag\left(0.02^2, \left(\frac{0.5\pi}{180}\right)^2, 0.02^2, \left(\frac{\pi}{180}\right)^2\right)$$

+Measurement matrix:

$$H = \begin{bmatrix} 0 & 0 & 1 & 0 & 0 & 0 & 0 & 0 & 0 & 0 & 0 & 0 \\ 0 & 0 & 0 & 0 & 0 & 0 & 0 & 1 & 0 & 0 & 0 & 0 \\ 0 & 0 & 0 & 0 & 0 & 0 & 0 & 0 & 0 & 0 & 1 & 0 \\ 0 & 0 & 0 & 0 & 0 & 0 & 0 & 0 & 1 & 0 & 0 & 0 \end{bmatrix}$$

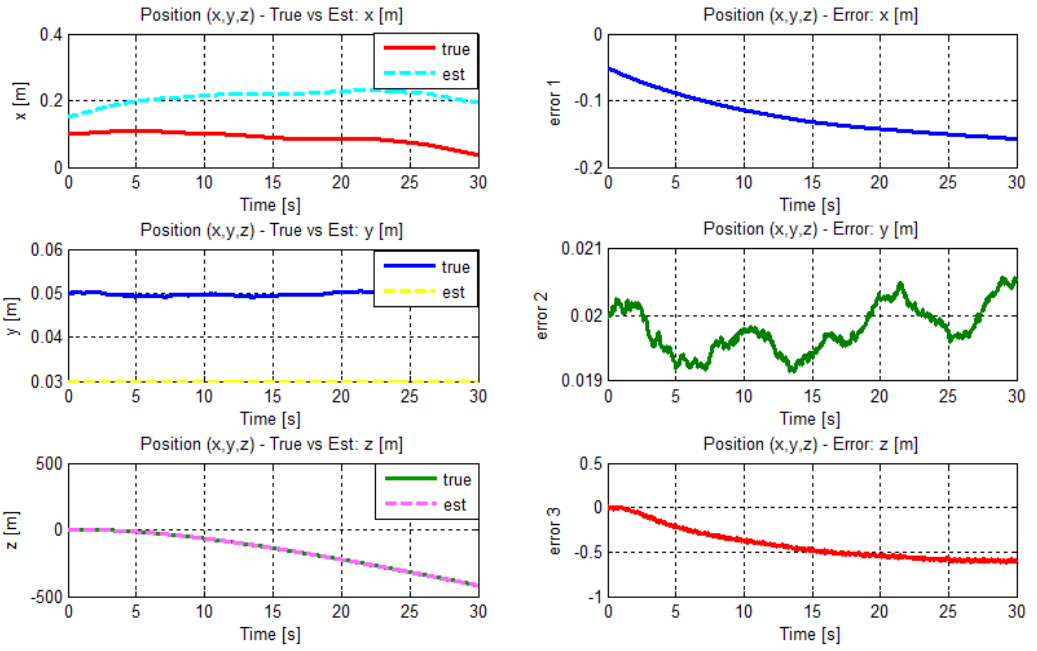


Figure 1. State estimation of position (x, y, z) using EKF and estimation errors

Figure 1 shows that the EKF accurately estimates the three position components (x, y, z). The error in the x-direction starts at approximately −0.18 m and decreases to −0.08(m) after 30(s). The error in the y-

direction remains very small, fluctuating within (0.019–0.021)(m). The z-channel exhibits larger initial error (≈ −0.5m), but it decreases to around −0.2(m) by the end of the simulation. These results indicate that EKF converges quickly and maintains stable, small errors for all three position components.

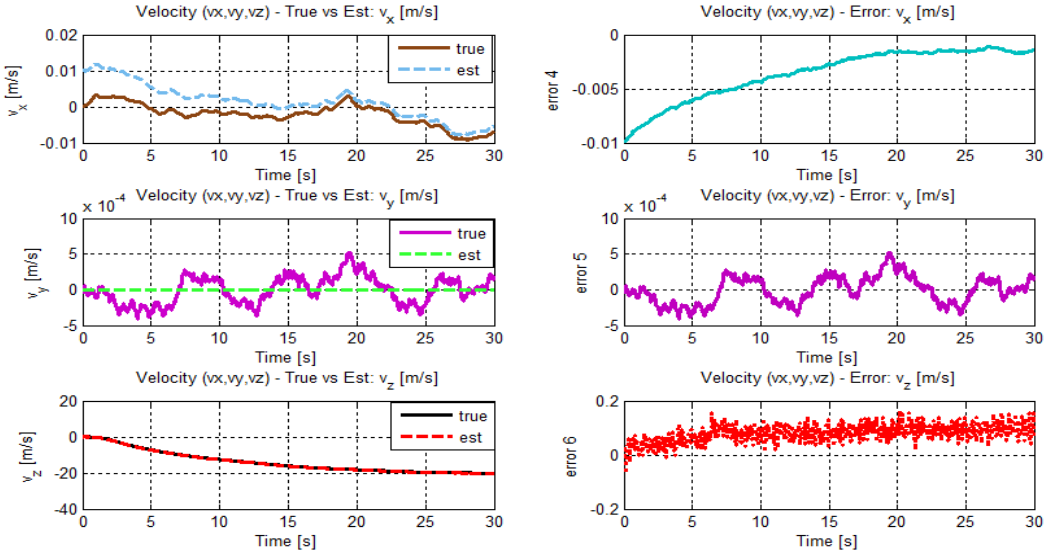


Figure 2. State estimation of velocity v_x, v_y, v_z using EKF and estimation errors

Simulation results show that EKF estimates all three velocity components accurately. In the v_x channel, the error starts at about −0.01(m/s), slightly increases to ≈ −0.003(m/s) by the end, with small oscillation amplitude. In the v_y channel, the value is nearly zero, with error fluctuating only within $\pm 5\times10^{-4}$(m/s), reflecting high accuracy and stability. In the v_z channel, although the absolute value is large (decreasing from 0 to about −50(m/s) due to heave control action), the error remains small (~±0.15(m/s)), showing that EKF successfully tracks fast variations in this channel.

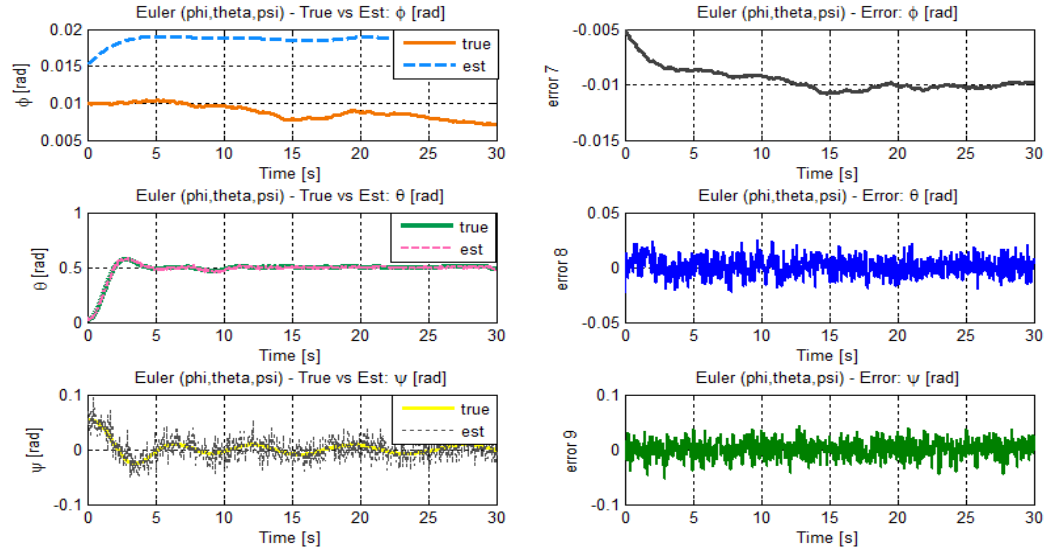


Figure 3. State estimation of Euler angles and estimation errors

Roll angle (ϕ) is estimated closely to the true value, with error decreasing from ~−0.005(rad) to below

−0.002(rad) after 30(s). Pitch angle (θ) has small error, randomly fluctuating around zero with amplitude ±0.02(rad), showing filter stability. Yaw angle (ψ) error fluctuates around zero with amplitude ±0.05(rad), demonstrating EKF accuracy even under rapid variations and noise. Overall, Euler angles are estimated with small errors compared to the true signals.

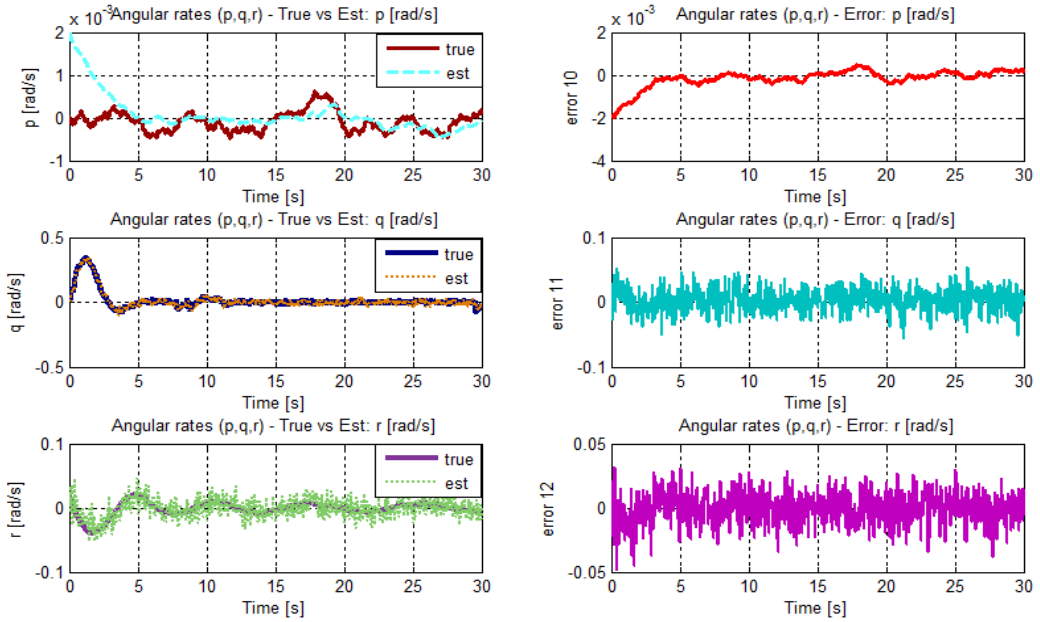


Figure 4. State estimation of angular rates p,q,r using EKF and estimation errors

Roll rate (p): estimated closely to the true value, with error around -2×10^{-3}(rad/s), stabilizing after ~5(s). Pitch rate (q): error is very small, within ±0.01(rad/s), indicating high accuracy and stability. Yaw rate (r): error fluctuates about ±0.05(rad/s), more variable due to yaw control action, but still within acceptable accuracy. In general, EKF maintains small angular rate errors relative to true values, ensuring reliable estimation for control.

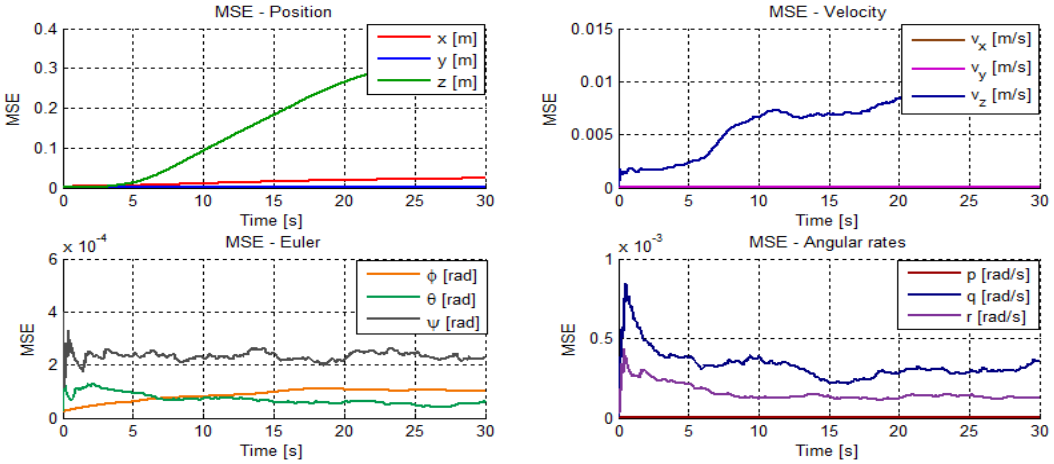


Figure 5. Mean Square Error (MSE) over time for position, velocity, Euler angles and angular rates

Position (x, y, z): X and Y coordinates maintain very small MSE (<0.01m^2), while Z increases gradually to ~0.27(m^2) after 30(s) due to vertical cumulative errors. Velocity (surge, sway, heave): v_x and v_y keep MSE

below 0.01 m^2/s^2, while v_z rises to ~0.012(m^2/s^2) due to control action and environmental disturbances. Euler angles (ϕ, θ, ψ): all angles show small MSE (<6×10^{-4} rad^2); yaw (ψ) has the largest but stabilizes after ~5(s). Angular rates (p, q, r): roll and pitch rates decrease quickly below 5×10^{-4}(rad^2/s^2), yaw rate fluctuates around 1×10^{-3}(rad^2/s^2).

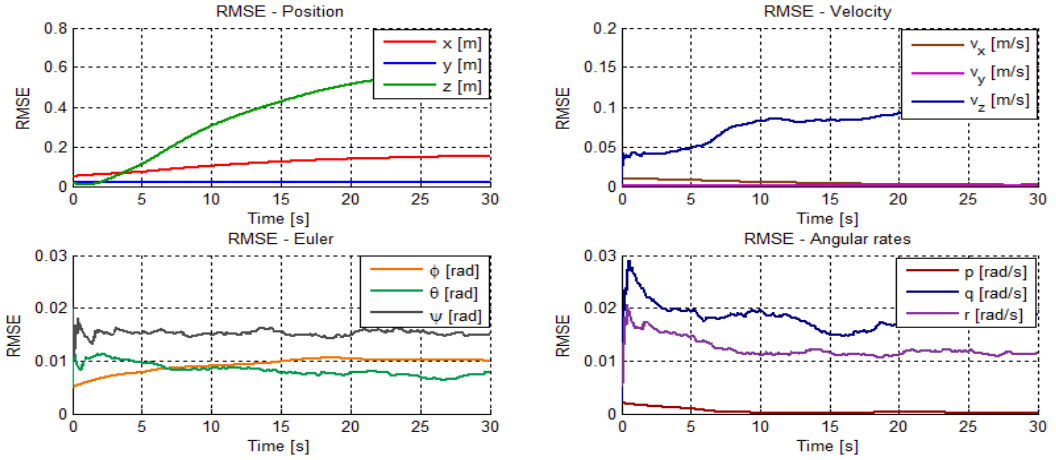


Figure 6. RMSE over time for position, velocity, Euler angles and angular rates

Position: RMSE of X and Y <0.15(m), while Z increases to ~0.52(m) at the end, reflecting higher vertical cumulative error. Velocity: RMSE of v_x and v_y <0.015(m/s); v_z increases to ~0.11(m/s) due to control and environmental effects. Euler angles: RMSE of ϕ and θ <0.015(rad); ψ fluctuates around 0.02(rad), stable after 5(s). Angular rates: roll rate RMSE <0.005(rad/s); pitch rate decreases from 0.025 to ~0.015(rad/s); yaw rate stays ~(0.02–0.025)(rad/s).

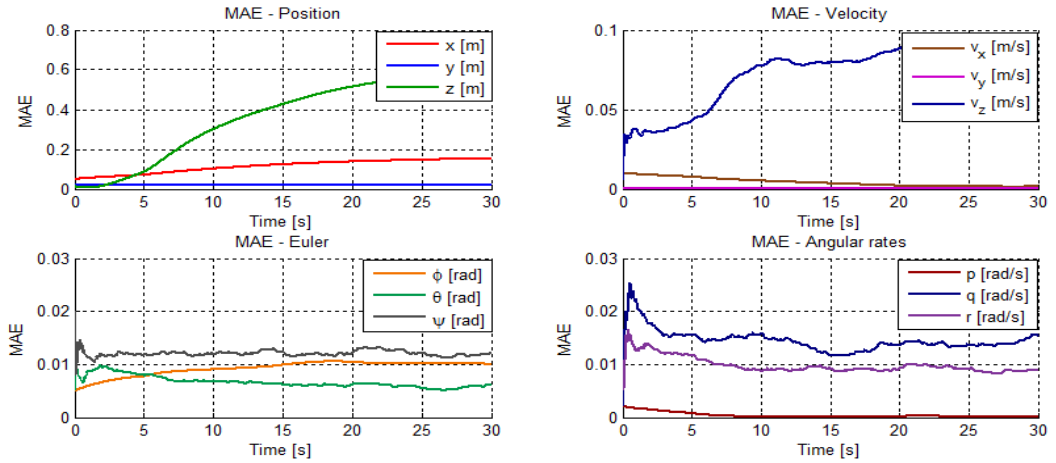


Figure 7. Mean Absolute Error (MAE) over time for position, velocity, Euler angles and angular rates

Position (x, y, z): The MAE of coordinate x and y remains small (< 0.12m), while the z-coordinate increases gradually and reaches about 0.5(m) at the end of the simulation. This reflects that the average error is larger in the vertical direction. Velocity (surge v_x, sway v_y, heave v_z): The MAE of v_x and v_y stays very low (< 0.008(m/s)). Meanwhile, v_z increases to approximately 0.08(m/s) due to the influence of control actions and environmental disturbances.

Euler angles: The MAE of roll (ϕ) and pitch (θ) both remain below 0.012(rad). The yaw angle (ψ)

ISSN 3048-8222 (Online) | www.ijsate.com | editor@ijsate.com

maintains around (0.018–0.02)(rad), stabilizing after the first few seconds of simulation. Angular rates: The MAE of roll rate (p) is less than 0.004(rad/s). The pitch rate (q) decreases gradually from about 0.02(rad/s) to ~0.012(rad/s). The yaw rate (r) fluctuates around (0.015–0.02(rad/s)), indicating that the filter maintains small average errors in estimating angular rates.

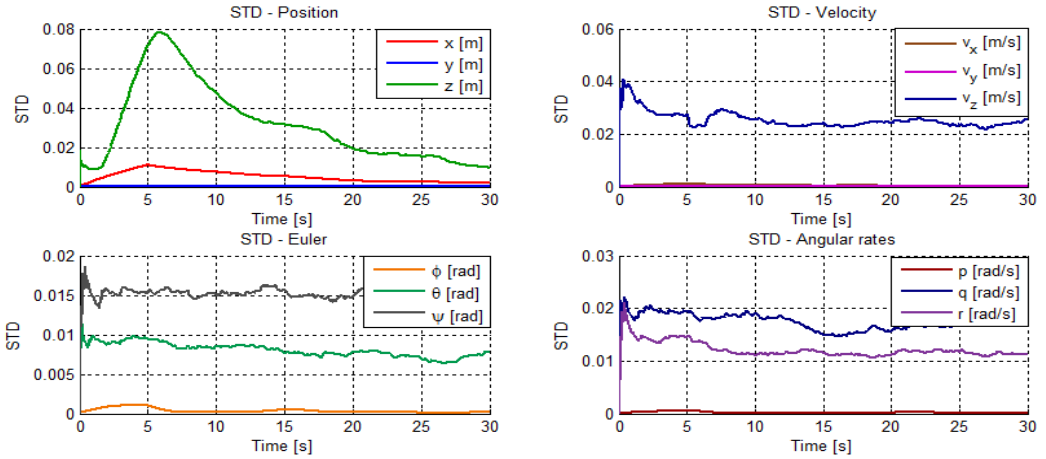


Figure 8. STD over time for position, velocity, Euler angles, and angular rates

Position (x, y, z): The STD of coordinates x and y remains very small (< 0.012(m)). The z-coordinate increases rapidly to about 0.075(m) at the 5th second, then gradually decreases to ~0.015(m) by the end of the simulation. This shows that the initial noise is gradually suppressed by the EKF. Velocity: The STD of v_x and v_y remains stable at a low level (< 0.002(m/s)). The STD of v_z is maintained at about (0.02–0.025)(m/s), reflecting fluctuations due to control actions and environmental disturbances. Euler angles: The STD of roll (ϕ) is the smallest (< 0.002(rad)). Pitch (θ) remains around (0.004–0.005)(rad). Yaw (ψ) is higher (~0.015(rad)) but stays stable over time. Angular rates: The STD of roll rate (p) remains below 0.002(rad/s). The pitch rate (q) decreases from 0.02(rad/s) to ~0.012(rad/s). The yaw rate (r) stays around (0.015–0.018)(rad/s), reflecting small and stable oscillations of angular rate estimates.

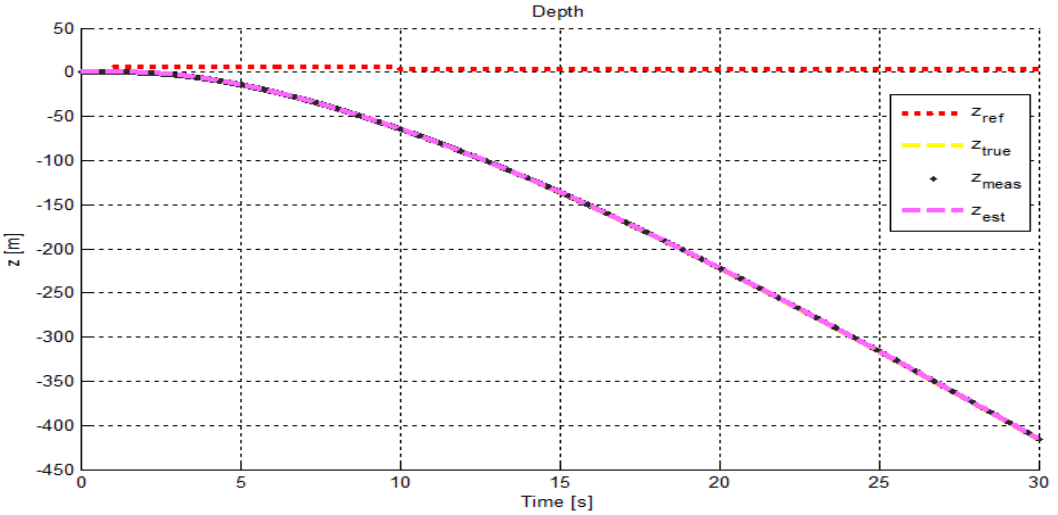


Figure 9. Depth z trajectory over time compared to reference, true value, measurement and estimation

The true depth (z_{true}) decreases gradually from 0(m) to about −450(m) after 30(s), matching the control

ISSN 3048-8222 (Online) | www.ijsate.com | editor@ijsate.com

trajectory. The measured depth (z_{meas}) follows the true value but contains small noise. The estimated depth from EKF (z_{est}) almost coincides with the true value, demonstrating the noise filtering and accurate estimation capability of EKF. The reference depth (z_{ref}) is kept fixed at 0(m), representing the case where the vehicle dives relative to the initial reference level.

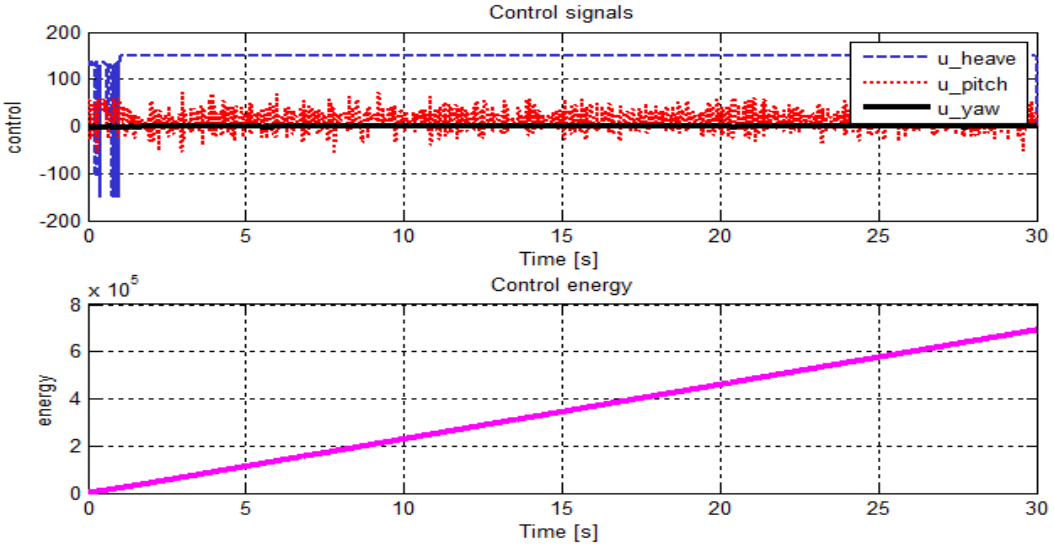


Figure 10. Control signals and control energy over time

The control signals include u_{heave}, u_{pitch} and u_{yaw} representing system response after applying the controller: u_{heave} maintains a large, nearly constant value (~100) after the initial transient phase, playing the dominant role in depth adjustment. u_{pitch}: oscillates around zero with significant amplitude and high frequency, reflecting the balancing of pitch motion. u_{yaw}: remains almost zero throughout the simulation, indicating that the system does not execute heading changes. The control energy increases linearly and reaches about 7×10^5 units at the end of the simulation, showing that the system consumes power steadily without abnormal energy oscillations.

4. Conclusion

This paper proposed a method that combines the EKF with SMC and a PD yaw controller in order to enhance the accuracy of state estimation and trajectory tracking of a 12-DOF underwater vehicle in complex disturbance environments. The EKF enables accurate estimation of position, velocity, Euler angles, and angular rates even when the measurement data are corrupted by Gaussian noise. Meanwhile, the SMC ensures robustness and strong disturbance rejection capability for the highly nonlinear depth and pitch control channels. The PD yaw controller allows the system to achieve fast and stable response in the yaw channel.

Simulation results demonstrate that the proposed method significantly reduces estimation errors compared with traditional methods, maintains system stability, and limits control energy consumption. The performance indices MSE, RMSE, MAE, and STD for all 12 state variables achieve low values, proving the effectiveness of the algorithm. In particular, the states estimated by EKF closely follow the true values even when the vehicle is simultaneously affected by ocean waves, currents, and random disturbances.

Declaration of Conflicting Interests

The authors declare no potential conflicts of interest with respect to the research, authorship and publication of this article.

Funding

The author received no financial support for the research, authorship and publication of this article.

References

[1] Chen, Q., Yuan, J., Dong, Z., Chai, Z., Wan, L. (2024), "Enhanced Control Strategies for Underactuated AUVs Using Backstepping Integral Sliding Mode Techniques for Ocean Current Challenges", *Journal of Marine Science and Engineering*, Vol.12, No.12, Article 2201. https://doi.org/10.3390/jmse12122201

[2] Mu, X. (2009), *Methods of Autonomous Formation Control and Cooperative Route Planning for Multi-missiles*, Beihang University, Beijing.

[3] K. Zhou, X. Wang, M. Tomizuka, W-B Zhang, and C-Y Chan (2002), "*A New Maneuvering Target Tracking Algorithm with Input Estimation*", American Control Conference, pp. 166-171

[4] Mohinder S. Grewal, Angus P. Andrews (2014): "*Kalman Filtering: Theory and Practice with MATLAB",* 4th Edition, John Wiley & Son, Inc

[5] Venkatesh Madyastha and Anthony Calise. (2005): "*An Adaptive Filtering Approach to Target Tracking"*. Proc. of the American Control Conference, pp. 1269-1274.

[6] Venkatesh Madyastha. (2009): "*Adaptive Estimation for Control of Uncertain Nonlinear Systems with Applications to Target Tracking*", VDM Verlag.

[7] Yong Ding, Chao Liu, Wenjie Li, Dandan Li, Wen Xu (2024), *"Intelligent Tracking Method for Aerial Maneuvering Target Based on Unscented Kalman Filter"*, Remote Sensing, Vol.16, No.17, 9/2024, pp.3301.

[8] Hongqiang Liu, Zhongliang Zhou, Haiyan Yang (2017*), "Tracking Maneuver Target Using Interacting Multiple Model-Square Root Cubature Kalman Filter Based on Range Rate Measurement"*, International Journal of Distributed Sensor Networks, Vol.13, No.12, 12/2017.

[9] Jinkun Cao, Jiangmiao Pang, Xinshuo Weng, Rawal Khirodkar, Kris Kitani (2022), *"Observation-Centric SORT: Rethinking SORT for Robust Multi-Object Tracking"*, arXiv preprint, 3/2022.

[10] Shet, R.M., Lakhekar, G.V., Iyer, N.C., et al. (2024), "Robust Path Following Control of AUVs Using Adaptive Super Twisting SOSMC", *Journal of Marine Science and Application*, Vol.23, pp.947–959, 2024. https://doi.org/10.1007/s11804-024-00471-w

[11] Wu, J., Liu, H., Li, B., Li, J., Li, M. (2024), "Precision trajectory control in underwater vehicle-manipulator systems using advanced sliding mode techniques and state estimation", *Ocean Engineering*, 2024. https://doi.org/10.1016/j.oceaneng.2024.120129

[12] Zhao, J., Zhang, Y., Li, S., Wang, J., Fang, L., Ning, L., Feng, J., Zhang, J. (2025), "An Improved Unscented Kalman Filter Applied to Positioning and Navigation of Autonomous Underwater Vehicles", *Sensors*, Vol.25, No.2, Article 551, 2025. https://doi.org/10.3390/s25020551

[13] Song, J., He, X. (2023), "Robust state estimation and fault detection for Autonomous Underwater Vehicles considering hydrodynamic effects", *Control Engineering Practice*, Vol.135, June 2023, 105497. https://doi.org/10.1016/j.conengprac.2023.105497